

# A quantitative measure of the degree of fibrillation of short reinforcing fibres

ARTHUR R. HENN,\* PHILLIP B. FRAUNDORF†  
*Monsanto Company, St. Louis, Missouri 63167, USA*

The degree of fibrillation of a reinforcing fibre can be viewed as the extent to which the fibre has partially been split longitudinally into thinner fibrils. Fibrillation provides larger surface area and is advantageous because it improves matrix-to-fibre coupling, oil absorption, thickening characteristics, and softness of the fibre. Fibrillation also allows for low bulk density and assists the mat-making capability of the fibre. A general means for quantifying the degree of fibrillation of a fibre is proposed. Taking the squared ratio of the fibre surface area determined by the BET method to that determined by measuring a sampling of many particles in a scanning electron micrograph, the technique for which is described herein, one has a quantitative, relatively simple method for calculating the degree of fibrillation. Results for calcium sodium metaphosphate fibre, a new inorganic fibre developed by Monsanto [1], milled glass fibre, and wollastonite fibre are reported and compared. Benefits of fibrillation are discussed.

## 1. Introduction and description of fibrillation

The "degree of fibrillation" of a reinforcing fibre characterizes the extent to which the fibre is partially split longitudinally into thinner, connected fibrils. The effect of fibrillation can partly be achieved also by having thinner fibres intertwined around larger-diameter fibres, thereby creating frayed-like areas on the larger fibres. Fibrillation is important because it can impart several beneficial features to a reinforcing fibre. For example, as a consequence of the greater surface area of a fibrillated fibre relative to a perfectly cylindrical one, matrix-to-fibre coupling is improved, as are the oil absorption [2] and thickening properties of the fibre. Another favourable feature of fibrillated fibres is that they tend to be softer and of lower bulk density than nonfibrillated fibres of the same diameter and aspect ratio (length to diameter ratio). The attendant high porosity of fibrillated fibres also allows for good thermal insulative characteristics. Furthermore, fibrillation assists the mat-making capability of the fibre. That is, well-formed mats of greater strength are more easily made with highly fibrillated fibres, such as cellulose or asbestos, than with unfibrillated fibres such as glass. Finally, it appears that fibrillation can be as important as fibre length in improving the tear strength of fibre-reinforced rubber compounds [3].

Asbestos is a well-known fibrillating fibre. The individual fibres of asbestos actually consist of very small, individual, stacked, easily separated, tubular fibrils [4]. Phosphate Fibre (PF), a calcium sodium

metaphosphate fibre developed by Monsanto Company [1], is another inorganic fibre that possesses a fibrillating nature. PF is fibrillatable because of an inherent tendency of the crystal lattice of calcium sodium metaphosphate to cleave preferentially along its *c*-axis, which is also the fibre axis [2]. Fig. 1 shows the fibrillated character of asbestos and PF [2]. This is to be compared to Figs 2 and 3, which exhibit scanning electron micrographs (SEM) of 1/16" milled glass and Nyad® G† wollastonite fibres, respectively. Note the obvious differences in fibre morphology, in particular, the almost complete absence of frayed ends on the glass and wollastonite fibres. Other fibres with fibrillating characteristics are the organic-based fibres such as cellulose, acrylic, aramid, and polyolefin fibres.

Given the functional significance of fibrillation, it is desirable to have a means of quantifying the average extent of fibrillation of a batch of fibres. In the asbestos industry, the degree of fibrillation (fiberization) is also called the degree of openness and is wholly associated with the surface area of the fibre [4]. Surface area is considered the most important parameter characterizing asbestos for any particular purpose. Hodgson [4] describes the degree of fiberization by saying that if a fibre of cross-sectional area  $A$  splits down to  $n$  fibres of average cross-sectional area  $A/n$ , then the degree of fiberization has been increased  $n$ -fold. Therefore, according to this description, the degree of fiberization can be quantified directly in terms of the measured surface area of the fibre. However, this simple measure is incomplete because total surface area alone cannot

\* Author to whom correspondence should be addressed.

† Also, Physics Department, University of Missouri-St. Louis, St. Louis, Missouri 63121.

‡ Nyad® is a registered trademark of Nyco, Willsboro, NY 12996-0368.

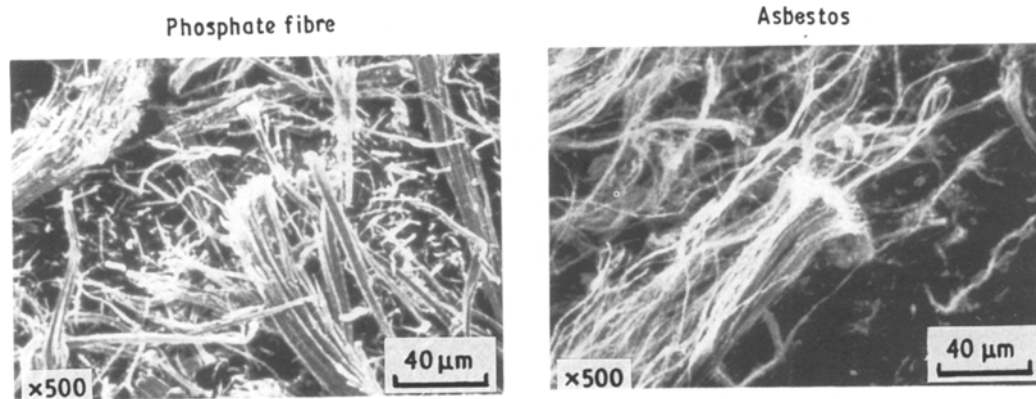


Figure 1 SEM close-ups of the fibrillated nature of PF and asbestos.

describe the degree of fibrillation unless one can be assured that the average lengths of the fibre batches being compared are the same — a highly unlikely occurrence. Without knowing the size and shape of the fibres, surface area alone has limited meaning with regard to fibrillation. One would not consider something like fumed silica to be more fibrillated than asbestos based solely on the fact that the surface area of fumed silica is 2–3 times as great as that of asbestos.

The present communication proposes that a simple and relatively accessible method for quantifying fibrillation for a batch of fibres is to compare the total surface area of the fibres, as determined by the Brunauer-Emmett-Teller (BET) measurement [5], to the area found by actual dimensional measurements on a large number of individual fibres (assumed to be perfect cylinders or rectangular prisms) observed on a scanning electron micrograph (SEM). If one defines the degree of fibrillation as the average effective number of separated fibrils per fibre, then, as shown in the next section, the squared ratio of these two types of surface areas gives such a number,  $\langle n \rangle$ ;

$$\langle n \rangle = (A_T/A_{ex})^2 \quad (1)$$

where  $A_T$  is the BET surface area, and  $A_{ex}$  is the external surface area determined from the SEM measurements, assuming perfectly shaped, single fibres.

The basis for equation (1) is that  $A_{ex}$ , calculated assuming perfect cylinders (or parallelepipeds) does not include the area contributions from fibrillation and other surface defects, whereas the BET surface area will include such contributions for all fibre cracks and pores accessible to the adsorbate gas (typically Kr or N<sub>2</sub>). Thus, the measure of fibrillation developed here is really an indicator of the deviation of the fibres from perfect fibre geometry and surface perfection. As a result, simple pores, holes, and nicks in a fibre, although not constituting true fibrillation, will contribute, in a small, but non-negligible extent, to the value of  $\langle n \rangle$ .

## 2. Model of fibrillation and derivation of equation 1

Defining the degree of fibrillation as the average effective number of fibrils into which a typical fibre is split, we may assume a simplified model in which a large parallelepiped fibre of length  $L$  and diameter  $D$  is

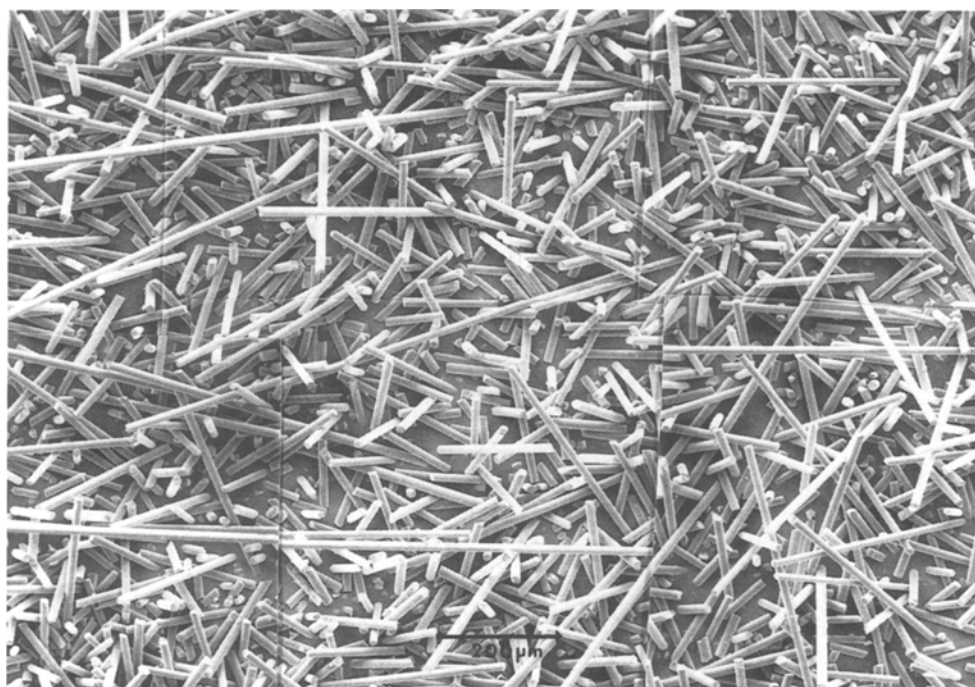


Figure 2 SEM of 1/16" milled glass fibre.

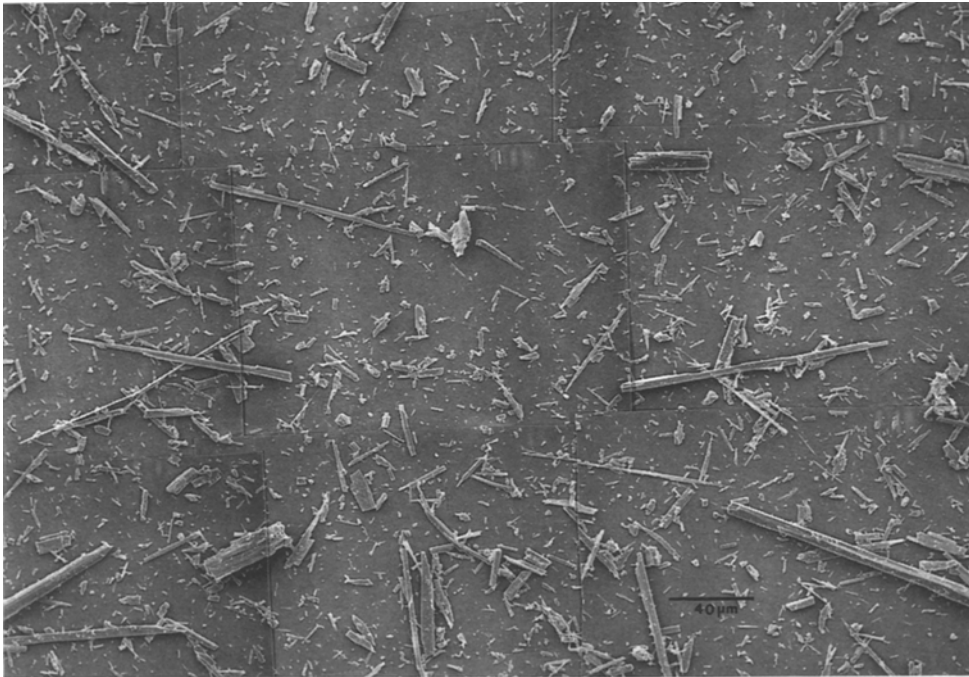


Figure 3 SEM of Nyad® G wollastonite fibre.

composed of an assembly of  $n$  smaller, similarly shaped fibrils of the same length  $L$ . The final result, Equation 1, holds equally well for cylinders and for parallelepipeds if one takes either the cross-sectional diagonal or side as the fibre diameter.

From Fig. 4, which is a model of a fibrillatable fibre one can see that the diameter,  $d$ , of the small fibrils is  $D/n^{1/2}$ . For a fibre of length  $L$  and diameter  $D$ , the external surface area is

$$A_{ex} = 4DL + 2D^2 \quad (2)$$

When the aspect ratio ( $L/D$ ) is greater than 10, the contribution to the area by the ends ( $2D^2$ ) is less than 5% and henceforth, for purposes of the derivation, will be ignored, although it was included in the actual measurement of the external fibre surface area,  $A_{ex}$ .

For fibre  $i$ , of length  $L$  and diameter  $D$ , the external surface  $A_{ex_i}$ , is then approximately

$$A_{ex_i} = 4D_i L_i \quad (3)$$

The total surface area of fibre  $i$ ,  $A_{T_i}$ , is composed of the sum of the surface areas of its  $n_i$  fibrils such that

$$A_{T_i} \simeq n_i(4d_i L_i + 2d_i^2) \quad (4)$$

$$= 4/n_i^{1/2} D_i L_i \quad (5)$$

where  $d_i = D_i/n_i^{1/2}$ , and the fibre end area contributions have been neglected. Taking the ratio of

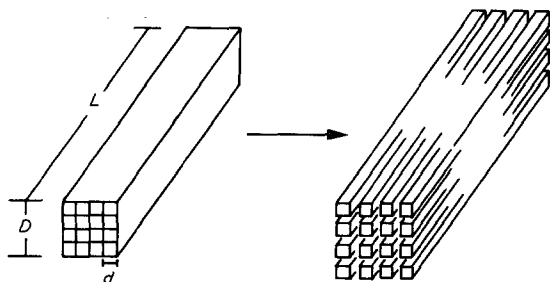


Figure 4 Model of a fibrillatable fibre. The diameter of the fibrillated fibre is expanded for purposes of illustration.

Equations 5 and 3 and solving for  $n_i$  gives

$$n_i = (A_{T_i}/A_{ex_i})^2 \quad (6)$$

This is the number of equally sized fibrils on fibre  $i$ . A perfectly formed fibre would have  $n = 1$ .

To get the average number of fibrils per fibre,  $\langle n \rangle$ , we sum over the number of fibres in an ensemble of fibres, say, a gram of fibres.

$$\langle n \rangle = \sum_{i=1}^N (A_{T_i}/A_{ex_i})^2 / N \quad (7)$$

where  $N$  is the number of fibres in the ensemble. Now,

$$\sum_{i=1}^N (A_{T_i}/A_{ex_i})^2 = N \left( \sum_{i=1}^N A_{T_i} / \sum_{i=1}^N A_{ex_i} \right)^2 \quad (8)$$

Therefore,

$$\langle n \rangle = \left( \sum_{i=1}^N A_{T_i} / \sum_{i=1}^N A_{ex_i} \right)^2 \quad (9)$$

The BET surface area,  $A_T$ , is defined as

$$A_T = \sum_{i=1}^N A_{T_i} / \sum_{i=1}^N w_i \quad (10)$$

where  $w_i$  is the weight of the  $i^{\text{th}}$  fibre (see Equation 16). The SEM surface area,  $A_{ex}$ , is similarly defined as

$$A_{ex} = \sum_{i=1}^N A_{ex_i} / \sum_{i=1}^N w_i \quad (11)$$

Dividing Equation 11 into Equation 10 and squaring the ratio gives

$$\left( \sum_{i=1}^N A_{T_i} / \sum_{i=1}^N A_{ex_i} \right)^2 = (A_T/A_{ex})^2 \quad (12)$$

Thus, comparing Equations 9 and 12, we see that the average number of fibrils per fibre is

$$\langle n \rangle = (A_T/A_{ex})^2 \quad (1)$$

which is just the squared ratio of the BET surface area

to the SEM area, and the desired result. Once again we note that  $\langle n \rangle$  for a perfectly shaped, nonfibrillated fibre is really  $\langle n \rangle = 1$ .

### 3. Measurement of $A_{ex}$ and other fibre dimensional data: discussion of microscopy and sampling technique

Measurements of individual fibre length and diameter were made from scanning electron micrographs of calibrated magnification, using a Zeiss-Kontron image processing system. The SEM images were first digitized into a  $512 \times 512$  pixel by a 256 grey-level display. Fibres were outlined on the digitized image with a computer-based pointing device, and the projected area ( $A_p$ ) and perimeter ( $P$ ) of each object were automatically measured and recorded. Fibre length and diameter, assumed here equal to projected fibre length and width, were then inferred using

$$L = (P/4) + ((P/4)^2 - A_p)^{1/2} \quad (13)$$

and

$$D = (P/4) - ((P/4)^2 - A_p)^{1/2} \quad (14)$$

assuming  $A_p = DL$  and  $P = 2(D + L)$  for each particle. The expressions (13) and (14), written in terms of perimeter and areas, were used because they permit estimation of projected fibre length and width even for cases in which the fibres are curved. For individual fibres, external surface areas and masses could be estimated using

$$A_{ex_i} = 4D_iL_i + 2D_i^2 \quad (15)$$

and

$$w_i = \rho L_i D_i^2 \quad (16)$$

where  $\rho$  is the true, or skeletal, density of the fibre. Total "external" surface area per gram of fibre ( $A_{ex}$ ) was calculated by Equation 11 with  $N$  equal to well over 200 fibres counted.

A few words of caution are in order here. If fibres occur over a wide range of sizes, as they do for PF, whose standard deviations in length and diameter typically are 50–100% of the respective mean, it is easily possible that one might count a large number of fibres without counting many from the subset of large fibres that contribute most of the mass. For the situation in which it is not known how the various particle

dimensions correlate with particle size, a reasonable estimate of the number of degrees of freedom (hence, the effective number of independent data points) that comprise the dimensional averages is not  $N$ , but  $N' = (\sum^N w_i)^2 / (\sum^N w_i^2)$  [6]. This number can be much smaller than  $N$  if only a few of the particles contribute appreciable mass. Our guideline in monitoring uncertainties has thus been as follows: if  $(1/N')^{1/2}$  is larger than the fractional uncertainty in a dimensional quantity one wishes to tolerate, then one should count more of the large fibres (for example, by sampling a larger area of dispersed particles) to obtain statistically more robust estimates of the abundance of massive particles in the set. Fortunately, the measurements of specific area described above are not nearly as sensitive to this problem as are measurements of number average dimension because the former are quotients of total surface area and total mass.

The statistics for the PF sampling from a very broad, non-Gaussian distribution of particle sizes gave  $N' = 43$ , which leads to a 15% uncertainty in the average dimensional quantities (see Table I). Nyad<sup>®</sup> G wollastonite also has a very broad particle size distribution. For our sampling of the wollastonite,  $N' = 14$ , leading to a 27% uncertainty in the means. As might be expected, the synthetic milled glass possesses more normal statistics. Although its length can vary over a fairly large range, partly due to breakage during processing, it has a smaller, more uniform range in diameter. Since particle mass depends on the square of the diameter, but only linearly on the length, the concern for statistical mass representation for milled glass is not as great as for PF. As it turns out, the uncertainty in the means for our milled glass sampling was about 11%.

### 4. Results and discussion

Both methods of surface area measurements were carried out on a standard sample of PF, 1/16" milled glass, and Nyad<sup>®</sup> G wollastonite fibres. The fibre samplings of the latter are pictured in Figs 2 and 3. Results of the surface area measurements and other dimensional data are listed in Table I. Observe that, although PF has a smaller external surface area, when fibrillation is taken into account, its total surface area exceeds that of the wollastonite fibre.

Even though the three types of fibres differ by a

TABLE I Dimensional data on PF, Nyad<sup>®</sup> G, and 1/16" milled glass fibre

	Nyad <sup>®</sup> G	PF	1/16" Milled Glass
SEM Number Average Diameter $\mu\text{m}$	1.2	3.2	13.7
Length $\mu\text{m}$	9	52	152
Aspect Ratio	9	17	11
Mass $\langle w \rangle$ , ng	0.11	2.4	68
SEM Mass-weighted Diameter $\mu\text{m}$	—	6.2	15.6
Length $\mu\text{m}$	—	128	336
Aspect Ratio	—	24	19.5
SEM Surface Area, $A_{ex}$ , $\text{m}^2 \text{g}^{-1}$	0.51	0.29	0.11
BET Surface Area, $A_T$ , $\text{m}^2 \text{g}^{-1}$	0.8	1.2	0.15
Average No. fibrils/fibre, $\langle n \rangle - 1$	1.5	16	0.9

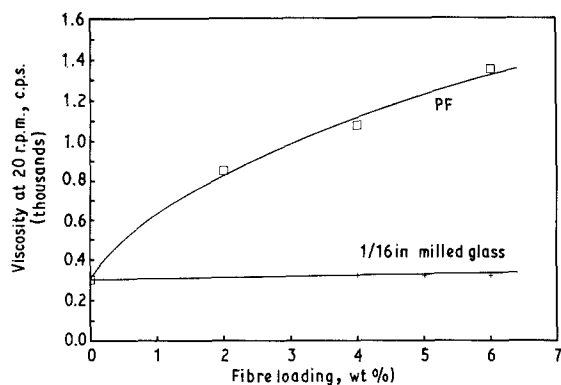


Figure 5 Comparison of the viscosity of an unsaturated polyester thermoset resin loaded with PF or 1/16" milled glass fibre at 23°C.

factor of up to ten or more in diameter and length, our definition and measurement of the degree of fibrillation allows for direct comparison. The results of the calculations show, not unexpectedly, that PF is more fibrillated than glass fibre and wollastonite, possessing over ten times as many fibrils per fibre as the milled glass and wollastonite fibres. Moreover, it should be realized that the fibrillation values for the glass fibre and wollastonite are actually even less than their listed values of 0.9 and 1.5 because microscopic examination reveals that it is only the nicks and cracks in the fibres, not fibrillation, that account for most of the deviation from perfect, smooth cylinders. Our method clearly shows that the wollastonite and milled glass fibre do not deviate greatly from perfect morphology and possess surfaces that are fairly free of defects. Such information is useful in its own right.

A benefit of fibrillation is evidenced in the thickening capability of PF. At higher fibre loadings, fibrillation allows for more mechanical interlocking among fibres, and this may contribute an additional mechanism by which fibrillated fibres act to increase the viscosity of a liquid. Figure 5 compares the viscosities (at 20 rpm) of an unsaturated polyester thermoset resin loaded with PF and with 1/16" milled glass fibre at room temperature. Even though the two types of fibre have values of  $A_{ex}$  that differ by less than a factor of three, at the same weight percent level, PF possesses a better than threefold thickening ability relative to the glass fibre due to fibrillation. Furthermore, the glass-loaded resin exhibits essentially no thixotropic character, whereas PF does impart some thixotropy to the resin [2]. This is consistent with the high oil absorption (ASTM D281) of PF, the value of which is over 300 [2, 8]. For comparison, the oil absorption of Nyad<sup>®</sup> G is 42 [7], and that of milled glass is less than 40<sup>†</sup>. The high oil absorption of PF is most likely due to the capillary action of its attached fibrils and pores.

Another benefit noted for fibrillated PF over unfi-

brillated glass fibre of similar aspect ratio is that PF tends to orient less than the glass fibre under low shear fields. As a consequence, composites made with PF will tend to have more isotropic properties not usually associated with glass filled systems [8-10].

## 5. Conclusions

A straightforward method for quantifying an important characteristic of reinforcing fibres, the degree of fibrillation, has been developed. The technique is conceptually simple and is generally applicable to all fibres for which an external surface area is obtainable from SEM pictures. Phosphate Fiber, an inorganic, reinforcing fibre originally developed by Monsanto [1], is compared to 1/16" milled glass fibre and wollastonite fibre and is shown to be considerably more fibrillated than either fibre, with attendant physical property advantages.

## Acknowledgements

The authors gratefully acknowledge Carol Pellegrin, for doing the SEM sizing measurements, and Dr. Marvin Crutchfield, for reviewing the manuscript and providing valuable comments and guidance.

## References

1. E. J. GRIFFITH, U.S. Patent 4346028, Asbestiform Crystalline Calcium Sodium or Lithium Phosphate Preparations and Compositions, August 1982.
2. A. R. HENN and M. M. CRUTCHFIELD, in "Advanced Materials Technology 1987", *Science of Advanced Materials and Process Engineering Series*, vol 32, edited by R. Carson, M. Burg, K. J. Kjoller and F. J. Riel (Society for the Advancement of Material and Processing Engineering, Covina, CA, 1987) pp. 1180-92.
3. L. K. ENGLISH, *Mater. Engng*, **105** (3) (1988) 14.
4. A. A. HODGSON, in "Asbestos - Properties, Applications and Hazards", vol. 1, edited by L. Michaels and S. S. Chissick (Wiley-Interscience, New York, 1979) Chap. 2.
5. A. W. Adamson in "Physical Chemistry of Surfaces", 3rd edn. (Wiley-Interscience, New York, 1976) Chap. XIV.
6. P. B. FRAUNDORF, "Microcharacterization of Stratosphere-collected Interplanetary Dust" Ph.D. Thesis, Washington University, St. Louis, MO, Appendix E (1980).
7. According to published Nyco technical literature, Nyad<sup>®</sup> G has an aspect ratio of 3-20 and a BET surface area of 0.8 m<sup>2</sup> g<sup>-1</sup>. Our SEM measurements give a number average aspect ratio of 9 ± 8, which agrees reasonably well. The oil absorption is given as 45 ml oil (100 g)<sup>-1</sup>; the density of linseed oil 0.93 g cc<sup>-1</sup>, giving 42 g (100 g)<sup>-1</sup>.
8. A. R. HENN, M. M. CRUTCHFIELD, B. F. MONZYK and J. A. HINKEBEIN, in "Handbook of Reinforcements for Plastics", edited by J. V. Milewski and H. S. Katz (Van Nostrand Reinhold, New York, 1987) Chap. 7.
9. B. F. MONZYK, *Plast. Compdg.* **9**(5) (1986) 42.
10. B. SILVERMAN, "Monsanto Technical Report" (1987).

Received 3 January  
and accepted 17 July 1989

<sup>†</sup> Unpublished results.